Real-time ghost free HDR video stream generation using weight adaptation based method

Mustapha Bouderbane, Pierre-Jean Lapray, Julien Dubois, Barthélémy Heyrman, Dominique Ginhac
Le2i UMR 6306, CNRS, Arts et Métiers, Univ. Bourgogne Franche-Comté, Dijon, France
first name.last name@u-bourgogne.fr

ABSTRACT

Temporal exposure bracketing is a simple and low cost technique to generate a high dynamic range (HDR) images. This technique is widely used to recover the whole dynamic range of a scene by selecting the adequate number of low dynamic range (LDR) images to be fused. Temporal exposure bracketing technique is introduced to be used for static scenes and it cannot be applied directly for dynamic scenes since camera or object motion in bracketed exposures creates ghosts in the resulting HDR image. In this paper we propose a HDR algorithm modification to remove ghost artifact and we present a real-time implementation of this method on a smart camera (HDR video stream 1280×1024 at $60fps$). We present experimental results to show the ghost removing efficiency of our implemented method.

Keywords

Exposure bracketing, ghost detection, real-time algorithm, high dynamic range, smart camera, tone mapping, weight adaptation, FPGA.

1. INTRODUCTION

Recently industries and researchers have trend toward a high dynamic range imaging generation, to extend the range of values that each pixel may represent. Nowadays, color images provided by a conventional camera, are represented with a byte per pixel for each of the red, green, and blue channels. Allowing about 16.7 millions of different colors which can be assigned to each pixel. This may seem an impressively large number at first, but it should be noted that there are still only 256 values per color channel of each pixel. Having just 256 values per channel is inadequate to represent the whole dynamic range of the scene. To overcome this limitation, the temporal exposure bracketing technique is widely used since it is a low-cost solution using a conventional image sensor. The high dynamic range image may be reconstructed using a HDR standard method in radiance domain [11, 12, 3], or by fusing LDR images directly in image domain producing a HDR-like image [15].

Temporal exposure bracketing solution is limited by the ghost artifact when applied directly for dynamic scenes. The ghost artifact is the presence of an object in different location in the generated HDR image caused by the object or camera motion when capturing the set of LDR images (LDR images are spaced in time token for the same scene). To overcome this limitation a large number of ghost removing techniques are proposed in the state of the art. Some of the ghost removal techniques keep one occurrence of the moving object: K.Jacobs proposes an entropy based method [6] which uses the measure of local entropy differences to detect regions affected by moving pixels, these regions are excluded from the HDR generation process. S.Kang presents an optical flow based method [7]. T. Grosch proposed a prediction based method [5], he has compared the measured pixel value with a predicted value using the CRF, all diverging pixels from their predicted values are excluded from the HDR generation process. A probabilistic motion pixel detection method proposed by An et al [1] and an SVD based methode proposed by Srikantha and Sidibé[14]. The other group of the ghost removing techniques suppressed all detected moving objects in the scene. Pixel order based method [13] which detects the moving pixels if their values in low exposure is greater then their values in higher exposure. Gradient based method [16] detects the moving pixels if the gradient changes its direction and gives low weights for moving pixels and large weights for static pixels using the gradient information (direction, magnitude). Khan et al proposed a density estimation based method [8] which is an iterative method that gives great weights for static pixels and small weights for moving pixels using density estimation. A large number of the mentioned ghost removal methods found in the state of the art are presented by a software implementation [6, 7, 1, 14, 16, 8] and their hardware implementation on a target FPGA circuit seems to be very complicated and would not respect the real-time condition.

To remove the ghost artifact we have combined the weighting function presented in [2] and the standard weight function of the high dynamic range generation using Debevec and Malik method [3]. The remainder of the paper is as follows: in the section 2 we present the proposed method to generate HDR with ghost removal and its software implementation results, section 3 is dedicated to the hardware implementation of the proposed method and its results. Finally, the section 4 concludes this paper and gives directions for future works.

ICDSC '16, September 12-15, 2016, Paris, France

DOI: http://dx.doi.org/10.1145/2967413.2967439

Table 1: Notations used in this paper

Notation	Definition
LDR	Low dynamic range
CRF	Camera response function
HDR	High dynamic range
Z_{ij}^k	Pixel value at the location i,j of the image k
E_{ij}	Radiance value at the location i,j
Z_{max}	Pixel maximum value
Z_{min}	Pixel minimum value
Z^{ref}	The reference LDR image
Δt_k	The exposure time of LDR image Z^k
$f^{-1}(Z)$	The inverse function of the CRF
$g(Z)$	The inverse logarithm function of the CRF
N	Number of LDR images

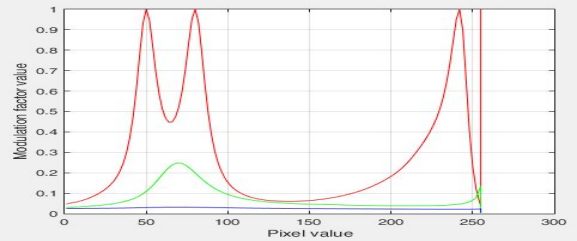

Figure 1: The weight modulation factor a function of the radiance deviation. Red curve is the factor for the closest radiance value of LDR images to the reference radiance value, the blue curve is the farthest value from the reference value and the green curve is for middle values.

2. HDR METHOD WITH GHOST REMOVAL

In this section we present our approach to suppress the ghost artifact. Our method repose on the modulation of weights, where we adjust pixel weights of the set of LDR images based on their deviation from pixels of the reference image using the weighting function given in the equation (1)[2]. Then the previous function is used as modulation factor to the standard weights (see equation (3)) given by Debevec and Malik[3].

$$w_{wfs}(Z_{ij}^k) = \frac{[a(Z_{ij}^{ref})]^2}{[a(Z_{ij}^{ref})]^2 + [(\frac{f^{-1}(Z_{ij}^k)}{\Delta t_k} - \frac{f^{-1}(Z_{ij}^{ref})}{\Delta t_{ref}})/\frac{f^{-1}(Z_{ij}^{ref})}{\Delta t_{ref}}]^2} \quad (1)$$

Where :
$E_{ij}^k = \frac{f^{-1}(Z_{ij}^k)}{\Delta t_k}$, $a(Z)$ is a function of the pixel value in the reference LDR image normalized to the [0,1] interval.

$$a(x) = \begin{cases} 0.058 + 0.68(x - 0.85) & if x \geq 0.85 \\ 0.04 + 0.12(1 - x) & if x < 0.85 \end{cases} \quad (2)$$

The equation (1), gives a higher factor for pixels whose recovered radiance value are closed to the recovered radiance of reference values and low factor for pixels whose radiance values diverge considerably from pixels radiance value of the reference image (see figure (1)) according to this fraction: $\frac{E_{ij}^k - E_{ij}^{ref}}{E_{ij}^{ref}}$.

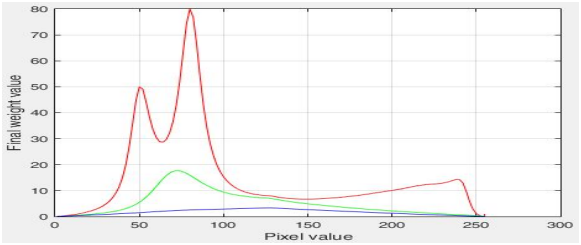

Figure 2: The final weight is a function of the radiance deviation and pixel value. Red curve is weights for the closest radiance value of LDR images to the reference radiance value, the blue curve is weights for farthest values from the reference value and green curve is weights for middle values.

To calculate final weighs to be used in the high dynamic range reconstruction, we multiply the standard weights calculated using the equation (3) by the modulation factor (see figure (2)).

$$w(z) = \begin{cases} z - Z_{min} \ for & z \leq \frac{1}{2}(Z_{min} + Z_{max}) \\ Z_{max} - z \ for & z > \frac{1}{2}(Z_{min} + Z_{max}) \end{cases} \quad (3)$$

$$W(Z_{ij}^k) = w(Z_{ij}^k) * w_{wfs}(Z_{ij}^k) \quad (4)$$

Using the equation (4), we give weight for a pixel according to its value compared to the well exposed value ($\frac{Z_{max} - Z_{min}}{2}$) in the same image using $w()$, and according to its deviation from a reference value in the reference image using $w_{wfs}()$.

To generate one HDR image, we fuse 3 LDR images in radiance domain using the algorithm given by Debevec and Malik [3]. This algorithm uses 3 functions to construct the high dynamic range radiance map, recovered camera response function (equation (6)), the weighting function (equation (3)) which is replaced in our case by $W()$ (equation (4)) and a function to combine different exposures (equation 5).

$$lnE_{ij} = \frac{\sum_{k=1}^{p} W(Z_{ij}^k)(g(Z_{ij}^k) - ln\Delta t_k)}{\sum_{k=1}^{p} W(Z_{ij}^k)} \quad (5)$$

$$g(Z_{ij}^k) = lnE_{ij}^k + ln\Delta t_k \quad (6)$$

2.1 The software implementation

We have implemented our method using Matlab software and tested it on different data bases to evaluate its performance and its weaknesses according to the motion magnitude. We used the stop motion to create a dynamic scene since this technique offers the possibility to variate the motion quantity in the scene and also create an HDR image of a static scene without ghosting artifact to be used as reference HDR image (see figure 3).

The first line of the LDR set of images is used to test the quality of the ghost removal for scenes containing small motions. The result HDR images are shown in figure (4). The HDR images generated using our method contain low ghost artifact (caused by the small motions of the train that

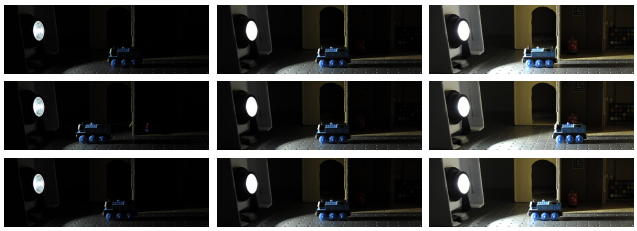

Figure 3: Set of LDR images, low exposure, medium and high exposure from left to right (small motion first line, big motion second line and static scene in the third line).

happened among the different exposures) comparing it to the result given using the standard method. The HDR range generation is done as well as using the standard method in static regions, where the three LDR images contribute efficiently in the HDR image result (see figure 6). More advanced details are shown in table (2).

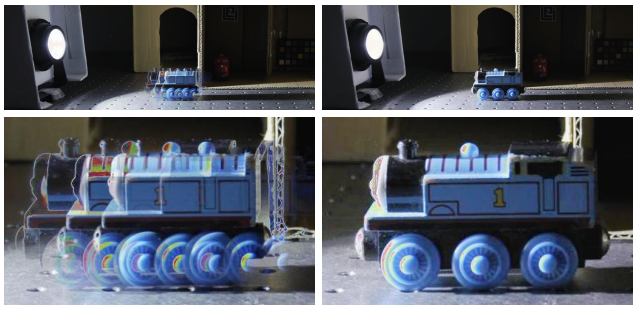

Figure 4: HDR images result, using standard method left and our method right.

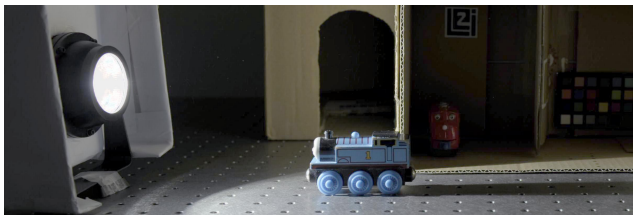

Figure 5: The reference HDR image created for static scene.

The PSNR, SSIM and other parameter values in table (2) are calculated between the reference image (see figure 5) ,the HDR image generated using the standard method and the HDR image generated using our method respectively. Values in the table (2) show that our method works well for scenes containing very small motion and produces better performance than the standard method. The figure (6), shows how LDR images contribute in the high dynamic range reconstruction, where colors represent main significant contribution of each exposure. In our case just 3 colors are used (the same number of exposures), blue color for the

Table 2: Results comparison for small motions

	Standard method	Our method
PSNR	+33.67 dB	+34.35 dB
SSIM	0.85	0.89
MSE	27.95	23.91
NRMSE	0.12	0.09
UQI	0.73	0.76

Figure 6: The contribution of the three LDR images in the HDR image using our method.

contribution of low exposure, cyan color for middle exposure and the green color for high exposure contribution.

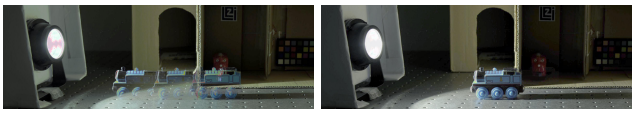

Figure 7: HDR images result, using standard method left and our method right.

The figure (7) shows how our method removes ghost artifact caused by the big motion of the moving train. The table (3) shows an advanced comparison between the standard Debevec and Malik HDR generation method and our HDR generation using the weighting function(see section 2) all using the same reference HDR image (5). Our method suppresses efficiently ghost artifact and gives good results in PSNR (it improves PSNR with more than 10 dB), SSIM, MSE and all other parameters.

3. HDR SMART CAMERA PRESENTATION

Our FPGA based smart camera is an upgraded version of the HDR-ARtiSt [10, 9]. This camera uses a Xilinx ML605 test platform board as a main board (see figure 8). The processing core is Xilinx Virtex-6 (xc6vlx240t). The ML605 board integrates a 512 MB SDRAM used to save 3 pictures with 3 different exposure times, then buffering these frames to the FPGA using a designed memory management unit. We added a PCB module to the Xilinx mother board. This PCB module integrates an E2V [4] (1280×1024 pixels) which is a low dynamic range color image sensor. It is used to capture frames with bracketed exposure technique at a maximum 4 LDR images per capture. We added 2 communication interfaces. Ethernet interface to send HDR images to a host computer with 2 modes, 32 bits images at 15 frames per second (fps) in full resolution (limited by the 1 Gb Ethernet interface bandwidth) or 8 bits tone mapped images at maximum frame rate allowed by the image sensor(60 fps) in full resolution. The DVI output interface is used to show HDR tone mapped frames on LCD monitor. All processing

Table 3: Results comparison for big motions

	Standard method	Our method
PSNR	+34.08 dB	+44.12 dB
SSIM	0.88	0.98
MSE	25.39	2.52
NRMSE	0.10	0.01
UQI	0.86	0.91

Table 4: Resources used by the hardware implementation

Component name	Number of component	percentage
Register	50399	16%
LUT	49193	29%
Slice	15705	41%
IO	210	35%
DSP48E1	20	2%
RAMB36E1	35	4%
BUFG	10	31%

algorithms (HDR generation, ghost removing, tone mapping and communication control interfaces) are implemented in hardware using VHDL description language.

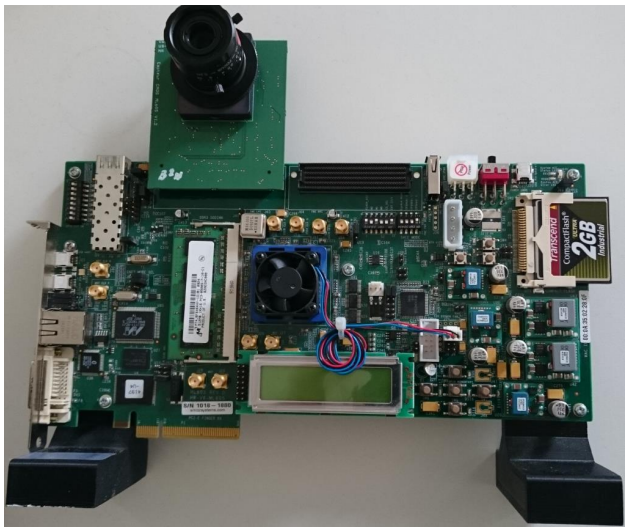

Figure 8: High dynamic range Xilinx FPGA based smart camera.

The implementation of the whole circuit (HDR generation, ghost removing, tone mapping and communication interfaces) is done using PlanAhead 14.7 software. The implemented circuit uses 29% of the Xilinx Virtex-6 (xc6vlx240t) FPGA, able to work with $114.247MHz$. More details are shown in table (4).

The figure (9) shows the result obtained using our smart camera integrating the proposed ghost removing method. Our camera generates HDR images of the same quality of the software off line generation using the standard method given by Debevec and Malik for static regions of the scene(see images of the background) with an efficient ghost removing for moving object (case of the moving guided car).

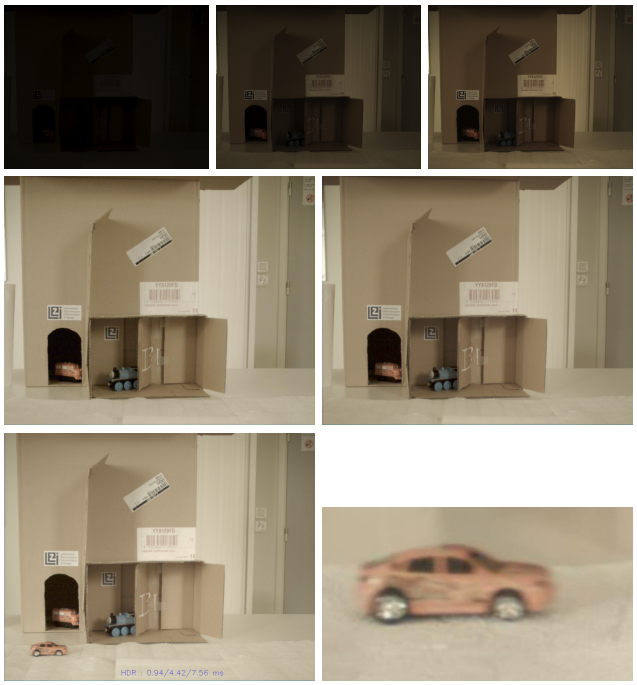

Figure 9: Set of LDR images of the scene background in the first line. Second line, soft generation of the HDR background image using the standard method in left and HDR background image captured by our smart camera in the right. The third line a HDR image of a real dynamic scene captured by our smart camera with a zoom on the moving car.

4. CONCLUSION

We have presented in this paper our work on the weight adaptation by combining the weighting function [2] with Debevec's weighting function[3] in the HDR reconstruction. Doing the mentioned modification in the high dynamic range generation process, we avoided ghosting artifact in real time and win more than 10 dB comparing the results of our method to the results obtained using the standard method all keeping a high reliability in the high dynamic range generation. The hardware implementation on a smart camera demonstrates that real-time processing can be reached with little logic consuming. The implemented method added a small latency of $1.03ms$ to the high dynamic generation caused by the uses of the floating point operators. The latency of 1.03 ms still acceptable to respect the real-time condition since our inter frame time is more than 16 ms.

5. REFERENCES

[1] J. An, S. J. Ha, and N. I. Cho. Probabilistic motion pixel detection for the reduction of ghost artifacts in high dynamic range images from multiple exposures. *EURASIP Journal on Image and Video Processing*, 2014(1):1–15, 2014.

[2] M. Bouderbane, J. Dubois, B. Heyrman, P.-J. Lapray, and D. Ginhac. Ghost removing for hdr real-time video stream generation. In *SPIE Photonics Europe*, pages 98970F–98970F. International Society for Optics and Photonics, 2016.

[3] P. E. Debevec and J. Malik. Recovering high dynamic range radiance maps from photographs. In *ACM SIGGRAPH 2008 classes*, page 31. ACM, 2008.

[4] e2v technologies. Ev76c661 BW and colour CMOS sensor, 2009. www.e2v.com.

[5] T. Grosch. Fast and robust high dynamic range image generation with camera and object movement. In *Proceedings of Vision, Modeling and Visualization Conference*, pages 277–284, 2006.

[6] K. Jacobs, C. Loscos, and G. Ward. Automatic high-dynamic range image generation for dynamic scenes. *IEEE Computer Graphics and Applications*, (2):84–93, 2008.

[7] S. B. Kang, M. Uyttendaele, S. Winder, and R. Szeliski. High dynamic range video. *ACM Transactions on Graphics (TOG)*, 22(3):319–325, 2003.

[8] E. A. Khan, A. Akyiiz, and E. Reinhard. Ghost removal in high dynamic range images. In *Image Processing, 2006 IEEE International Conference on*, pages 2005–2008. IEEE, 2006.

[9] P.-J. Lapray, B. Heyrman, and D. Ginhac. Hardware-based smart camera for recovering high dynamic range video from multiple exposures. *Optical Engineering*, 53(10):102110, 2014.

[10] P.-J. Lapray, B. Heyrman, and D. Ginhac. Hdr-artist: an adaptive real-time smart camera for high dynamic range imaging. *Journal of Real-Time Image Processing*, pages 1–16, 2014.

[11] T. Mitsunaga and S. K. Nayar. Radiometric self calibration. In *Computer Vision and Pattern Recognition, 1999. IEEE Computer Society Conference on.*, volume 1. IEEE, 1999.

[12] M. A. Robertson, S. Borman, and R. L. Stevenson. Estimation-theoretic approach to dynamic range enhancement using multiple exposures. *Journal of Electronic Imaging*, 12(2):219–228, 2003.

[13] D. Sidibé, W. Puech, and O. Strauss. Ghost detection and removal in high dynamic range images. In *Signal Processing Conference, 2009 17th European*, pages 2240–2244. IEEE, 2009.

[14] A. Srikantha, D. Sidibé, and F. Mériaudeau. An svd-based approach for ghost detection and removal in high dynamic range images. In *Pattern Recognition (ICPR), 2012 21st International Conference on*, pages 380–383. IEEE, 2012.

[15] F. V. R. Tom Mertens, Jan Kautz. Exposure fusion. Technical report, Hasselt University EDM transationale Universiteit Limburg Belgium, University College London UK, 2007.

[16] W. Zhang and W.-K. Cham. Gradient-directed composition of multi-exposure images. In *Computer Vision and Pattern Recognition (CVPR), 2010 IEEE Conference on*, pages 530–536. IEEE, 2010.